

A New Polymorph of Lithium Zinc Phosphate with the Cristobalite-Type Framework Topology

Xianhui Bu, Thurman E. Gier, and Galen D. Stucky

Department of Chemistry, University of California, Santa Barbara, California 93106

Received August 27, 1997; in revised form January 20, 1998; accepted January 27, 1998

A new form of lithium zinc phosphate has been prepared under high temperature and high pressure. The structure consists of lithium, zinc, and phosphorus atoms tetrahedrally coordinated to oxygen atoms. The three-dimensional framework structure can be described as belonging to the family of stuffed cristobalite structures with zinc and phosphorus atoms as framework tetrahedral atoms and lithium as extra-framework, charge-balancing cations. The cristobalite framework is derived from that of the diamond type, with the insertion of oxygen atoms between tetrahedral atoms. It is constructed from the stacking of hexagonal layers in the ABC sequence and consists of six-ring channels propagating in directions significantly offset from the stacking directions of layers. Crystal data for LiZnPO_4 : $M = 167.28$, space group Cc (No. 9), $a = 17.2962(1) \text{ \AA}$, $b = 9.7753(1)$, $c = 16.1989(2) \text{ \AA}$, $\beta = 98.953(1)^\circ$, $V = 2705.47(5) \text{ \AA}^3$, $Z = 32$, $D_c = 3.285 \text{ g cm}^{-3}$, $\text{MoK}\alpha$, $\mu = 7.573 \text{ mm}^{-1}$, $2\theta_{\text{max}} = 56.52^\circ$, $R(F) = 2.35\%$ for 506 parameters and 6219 reflections with $I > 2\sigma(I)$. © 1998 Academic Press

INTRODUCTION

For many years, silica in all of its several polymorphs has been a material of interest to geologists, crystallographers etc. concerned with the chemical and physical properties of solids (1). In these materials, tetrahedral silicon atoms can be replaced partially or totally by other tetrahedrally coordinated elements to give a variety of structural derivatives (2). Quartz, cristobalite, and tridymite have small cages and narrow channels and can all be “stuffed” with “extra” cations, providing that the restraint of charge balance is observed (3).

We have been interested for some time in the synthesis and crystal growth of compounds with structures derived from various forms of silica with the goal of determining physical properties pertinent to electro-optics, piezo-electricity, and luminescence. The family of materials with the general formula of ABCX_4 (A, B, and C are cations; X is an anion) have a rich substitution chemistry and a variety of structural types (4). This makes it possible to fine-tune

a specific physical property either to design a new useful material or to study structure–property correlations for a series of related materials. An added advantage is that many of these materials are noncentrosymmetric (4). This makes them attractive for the study of several important physical properties, such as the second harmonic generation.

The divalent metal phosphate system is also our recent focus in the synthesis of new zeolite analog structures (5–7). The study of these relatively dense phases helps us understand the chemistry of pertinent systems and provides useful guidance in the designed synthesis of new zeolitic materials (8–11).

EXPERIMENTAL

Hydrothermal Synthesis

LiH_2PO_4 (1.04g), 0.16g of ZnO, and 0.40g H_2O were sealed in a small gold tube (0.64 cm in diameter and 6.4 cm in height) and heated in a high temperature bomb (Tempres) to about 873 K at 30,000 psi for 40 h. The system was slowly cooled to about 473 K over 40 h, and then furnace cooled. After recovery via standard filtration and drying techniques (pH = 2.0), masses of small crystals (100% yield) suitable for structure determination were obtained. The X-ray powder diffraction pattern collected between 3° and 60° did not reveal any impurity phase. The measurement of second harmonic generation (SHG) of ground powder was carried out at $1.064 \mu\text{m}$ using a system similar to that described by Dougherty and Kurtz (12) and gave a value 1.2 times that of quartz, indicating an acentric structure.

Single Crystal Diffraction

A crystal was glued to a thin glass fiber with epoxy resin and mounted on a Siemens Smart CCD diffractometer equipped with a normal focus, 2.4 kW sealed tube X-ray source (MoK α radiation, $\lambda = 0.71073 \text{ \AA}$) operating at 50 kV and 40 mA. A full sphere of intensity data were collected in 2082 frames with ω scans (width of 0.30° and exposure time

of 30 sec. per frame). The empirical absorption correction was based on the equivalent reflections, and other possible effects, such as absorption by the glass fiber, were simultaneously corrected. The structure was solved by direct methods followed by successive difference Fourier methods. All calculations were performed using SHELXTL running on Silicon Graphics Indy 5000. Final full-matrix refinements were against F^2 and included secondary extinction correction and anisotropic thermal parameters for all atoms. Parameter shifts in the final least-squares cycle were smaller than 0.03σ . The crystallographic results are summarized in Table 1, while the atomic coordinates and selected bond distances are listed in Tables 2 and 3, respectively.

RESULTS AND DISCUSSION

Description of the Framework Structure

The new form of lithium zinc phosphate (denoted as $\text{LiZnPO}_4\text{-CR1}$) has the same framework topology as that of cristobalite. The cristobalite framework topology is identical to that of the diamond framework, but with additional oxygen atoms inserted between a pair of tetrahedral atoms. The diamond-type framework is one of the most common tetrahedral frameworks, and many complex frameworks can be reduced to the diamond-type framework when a cluster of tetrahedral atoms is topologically replaced with a single tetrahedral atom. The faujasite-type framework, which is the framework topology for commercially important molecular sieves, zeolites X and Y, is one such example (13). Some other frameworks can also be considered as the

TABLE 1
A Summary of Crystal Data and Refinement Results

Formula	LiZnPO_4
Habit	translucent prism
Color	clear
Size (μm^3)	$13.3 \times 13.3 \times 26.6$
a (Å)	17.2962(1)
b (Å)	9.7753(1)
c (Å)	16.1989(2)
β (°)	98.953(1)
V (Å ³)	2705.47(5)
Z	32
Space group	Cc (No. 9)
$2\theta_{\text{max}}$ (°)	56.52
Total data	13471
Unique data	6219
Parameters	506
$R(F)$ (%) ^a	2.35
$R_w(F^2)$ (%) ^b	5.98
GOF	1.07

^a $R(F) = \sum ||F_o| - |F_c|| / \sum |F_o|$ with $F_o > 4.0 (F)$.

^b $R_w(F^2) = [\sum [w(F_o^2 - F_c^2)]^2 / \sum [w(F_o^2)]^2]^{1/2}$ with $F_o > 4.0\sigma(F)$. $w = 1 / [\sigma^2(F_o^2)]$.

TABLE 2
Atomic Coordinates ($\times 10^4$) and Equivalent Isotropic Displacement Parameters (Å² $\times 10^3$)

	x	y	z	$U(\text{eq})$
Zn(1)	5756(1)	6921(1)	8723(1)	9(1)
Zn(2)	8263(1)	4450(1)	8730(1)	9(1)
Zn(3)	6645(1)	6603(1)	6222(1)	9(1)
Zn(4)	6077(1)	1621(1)	8726(1)	9(1)
Zn(5)	4429(1)	9383(1)	6211(1)	10(1)
Zn(6)	4169(1)	4091(1)	6208(1)	10(1)
Zn(7)	3570(1)	4111(1)	8711(1)	9(1)
Zn(8)	6955(1)	1851(1)	6216(1)	9(1)
P(1)	5084(1)	4065(2)	8090(1)	7(1)
P(2)	7605(1)	1582(2)	8092(1)	7(1)
P(3)	3527(1)	6868(2)	5583(1)	6(1)
P(4)	7303(1)	6872(2)	8112(1)	7(1)
P(5)	8232(1)	6582(2)	5602(1)	7(1)
P(6)	9814(1)	4375(2)	8107(1)	7(1)
P(7)	5751(1)	4073(2)	5602(1)	7(1)
P(8)	6010(1)	9364(2)	5586(1)	7(1)
O(1)	5163(2)	5610(4)	7949(2)	11(1)
O(2)	5013(2)	8387(4)	8850(2)	11(1)
O(3)	6141(2)	6237(4)	9829(2)	12(1)
O(4)	6620(2)	7810(4)	8269(2)	10(1)
O(5)	7663(2)	3132(4)	7967(2)	11(1)
O(6)	9134(2)	5298(4)	8270(2)	10(1)
O(7)	7525(2)	5916(4)	8876(2)	12(1)
O(8)	8628(2)	3772(4)	9840(2)	12(1)
O(9)	7052(2)	5945(5)	7337(2)	12(1)
O(10)	7400(2)	6012(4)	5485(2)	11(1)
O(11)	6279(2)	8489(4)	6374(2)	11(1)
O(12)	5688(2)	5622(4)	5737(2)	10(1)
O(13)	7208(2)	1242(4)	8854(2)	13(1)
O(14)	5521(2)	248(4)	7983(2)	11(1)
O(15)	5905(2)	3410(4)	8202(2)	12(1)
O(16)	5803(2)	8380(4)	4842(2)	12(1)
O(17)	9594(2)	3496(4)	7317(2)	11(1)
O(18)	5306(2)	10213(4)	5739(2)	10(1)
O(19)	3745(2)	10939(5)	6366(2)	10(1)
O(20)	4180(2)	7856(4)	5415(2)	10(1)
O(21)	4535(2)	3441(5)	7351(2)	12(1)
O(22)	8197(2)	8147(4)	5729(2)	12(1)
O(23)	3817(2)	5952(5)	6342(2)	12(1)
O(24)	4922(2)	3456(4)	5495(2)	11(1)
O(25)	4703(2)	3773(4)	8873(2)	12(1)
O(26)	3002(2)	2753(4)	7958(2)	10(1)
O(27)	3305(2)	5911(4)	4835(2)	12(1)
O(28)	3424(2)	5944(4)	8209(2)	10(1)
O(29)	7078(2)	987(5)	7316(2)	12(1)
O(30)	2817(2)	7706(4)	5746(2)	10(1)
O(31)	6286(2)	3448(5)	6360(3)	13(1)
O(32)	6670(2)	333(4)	5422(2)	9(1)
Li(1)	8875(8)	6831(9)	7480(8)	16(2)
Li(2)	4205(5)	6612(10)	7475(5)	11(2)
Li(3)	6667(5)	4074(10)	7471(6)	11(2)
Li(4)	6395(5)	9392(12)	7462(5)	13(2)
Li(5)	7271(5)	4130(11)	4979(6)	12(2)
Li(6)	4762(5)	8359(11)	9971(6)	13(2)
Li(7)	5053(5)	6922(10)	4971(6)	13(2)
Li(8)	2565(6)	4447(10)	4965(6)	13(2)

Note. $U(\text{eq})$ is defined as one third of the trace of the orthogonalized U_{ij} tensor.

TABLE 3
Selected Bond lengths (Å)

Zn(1)–O(3)	1.931(4)	Zn(1)–O(2)	1.958(4)
Zn(1)–O(1)	1.966(4)	Zn(1)–O(4)	1.967(4)
Zn(2)–O(8)	1.928(4)	Zn(2)–O(7)	1.958(4)
Zn(2)–O(6)	1.966(4)	Zn(2)–O(5)	1.966(4)
Zn(3)–O(9)	1.943(4)	Zn(3)–O(12)	1.968(3)
Zn(3)–O(11)	1.977(4)	Zn(3)–O(10)	1.988(3)
Zn(4)–O(16)	1.940(4)	Zn(4)–O(15)	1.948(4)
Zn(4)–O(14)	1.953(4)	Zn(4)–O(13)	1.968(4)
Zn(5)–O(19)	1.967(4)	Zn(5)–O(17)	1.971(4)
Zn(5)–O(20)	1.975(4)	Zn(5)–O(18)	1.975(4)
Zn(6)–O(23)	1.942(4)	Zn(6)–O(21)	1.966(4)
Zn(6)–O(22)	1.968(4)	Zn(6)–O(24)	1.970(4)
Zn(7)–O(27)	1.946(4)	Zn(7)–O(26)	1.960(4)
Zn(7)–O(25)	1.963(4)	Zn(7)–O(28)	1.969(4)
Zn(8)–O(29)	1.953(4)	Zn(8)–O(30)	1.964(4)
Zn(8)–O(32)	1.975(4)	Zn(8)–O(31)	1.979(4)
P(1)–O(21)	1.534(4)	P(1)–O(1)	1.537(4)
P(1)–O(15)	1.542(4)	P(1)–O(25)	1.544(4)
P(2)–O(28)	1.533(4)	P(2)–O(5)	1.534(4)
P(2)–O(13)	1.539(4)	P(2)–O(29)	1.547(4)
P(3)–O(30)	1.532(4)	P(3)–O(27)	1.532(4)
P(3)–O(23)	1.540(4)	P(3)–O(20)	1.542(4)
P(4)–O(26)	1.536(4)	P(4)–O(4)	1.547(4)
P(4)–O(7)	1.551(4)	P(4)–O(9)	1.555(4)
P(5)–O(10)	1.527(4)	P(5)–O(19)	1.541(4)
P(5)–O(8)	1.541(4)	P(5)–O(22)	1.547(4)
P(6)–O(14)	1.531(4)	P(6)–O(6)	1.538(4)
P(6)–O(17)	1.539(4)	P(6)–O(2)	1.539(4)
P(7)–O(12)	1.536(4)	P(7)–O(24)	1.540(4)
P(7)–O(3)	1.543(4)	P(7)–O(31)	1.544(4)
P(8)–O(18)	1.526(4)	P(8)–O(32)	1.537(4)
P(8)–O(16)	1.541(4)	P(8)–O(11)	1.546(4)
Li(1)–O(21)	1.975(13)	Li(1)–O(19)	1.986(13)
Li(1)–O(26)	2.013(13)	Li(1)–O(6)	1.975(11)
Li(2)–O(17)	1.991(10)	Li(2)–O(1)	1.974(9)
Li(2)–O(23)	1.963(10)	Li(2)–O(28)	2.040(10)
Li(3)–O(5)	2.008(10)	Li(3)–O(31)	1.918(10)
Li(3)–O(9)	1.970(10)	Li(3)–O(15)	2.012(10)
Li(4)–O(29)	1.993(11)	Li(4)–O(14)	2.022(10)
Li(4)–O(11)	1.953(10)	Li(4)–O(4)	2.023(11)
Li(5)–O(10)	2.012(11)	Li(5)–O(7)	1.905(10)
Li(5)–O(3)	1.965(10)	Li(5)–O(30)	2.002(11)
Li(6)–O(24)	1.968(11)	Li(6)–O(8)	1.982(10)
Li(6)–O(18)	2.005(11)	Li(6)–O(2)	1.932(10)
Li(7)–O(16)	1.959(10)	Li(7)–O(12)	1.984(10)
Li(7)–O(25)	1.912(10)	Li(7)–O(20)	1.994(10)
Li(8)–O(13)	1.931(10)	Li(8)–O(22)	1.980(10)
Li(8)–O(32)	2.013(10)	Li(8)–O(27)	1.952(10)

diamond-type framework, but with “defects”. The tetrahedral-triangular framework structure of a hydrated sodium zincocarbonate belongs to this class (14). Another interesting example is an open-framework vanadium phosphate, in which large cavities are connected in a manner that is topologically equivalent to the arrangement of tetrahedral atoms in the diamond-type framework (15).

A distinctive structural feature of the diamond-type topology is the presence of adamantane cages consisting of ten tetrahedral centers (Fig. 1). The number of adamantane cages is equal to the number of tetrahedral atoms on the framework. Thus for $\text{LiZnPO}_4\text{-CR1}$, there are two adamantane cages for each lithium atom. The distribution of lithium atoms in adamantane cages is not random, though. One type of adamantane cage, which consists of six zinc cations and four phosphorus cations, is more negatively charged than the other type, which consists of four zinc cations and six phosphorus cations. As expected, lithium cations are located in the more negatively charged cages (6 Zn^{2+} and 4 P^{5+} , Fig. 1). A similar situation exists in $[\text{N}(\text{CH}_3)_4] \text{LiZn}(\text{CN})_4$, which has a diamond-type framework with lithium and zinc as tetrahedral centers (16).

The diamond-type topology is ideally cubic. But the adamantane cage formed from ZnO_2^{2-} and PO_2^+ tetrahedra is too large for lithium cations to sit at the cage center. Thus, the zinc phosphate framework undergoes certain distortions to provide the optimum coordinations for lithium cations. This results in a symmetry reduction from cubic to monoclinic. The relationship between the size of extra-framework cations and the type of framework topologies in ABCO_4 -type structures has been discussed in detail elsewhere (4).

The diamond-type topology can be considered as built from hexagonal layers (six tetrahedral atoms in a ring) stacked along any one of four crystallographic directions (Fig. 2). These four crystallographic directions are very easy to visualize in an ideal diamond framework. They correspond to the four body-diagonal directions in a cubic unit cell and are related to the fact that there are four hexagonal rings for each adamantane cage. However, in a distorted structure, not all of these directions are easily discernible because of the differing extent of ruggedness of the four

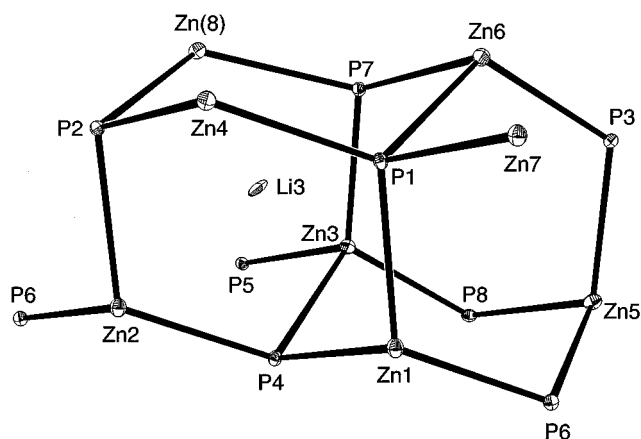


FIG. 1. The ORTEP (50%) drawing of two adjacent adamantane cages, one occupied by a lithium cation and the other empty. Oxygen atoms are omitted for clarity.

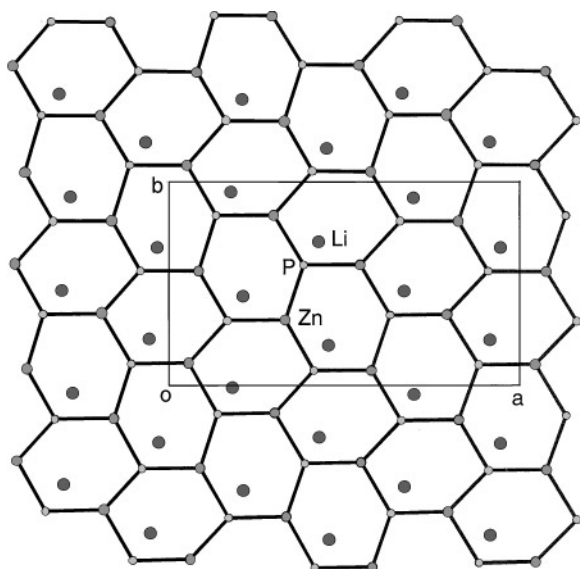


FIG. 2. The tetrahedral atom connectivity diagram showing an infinite hexagonal sheet perpendicular to the crystallographic c -axis.

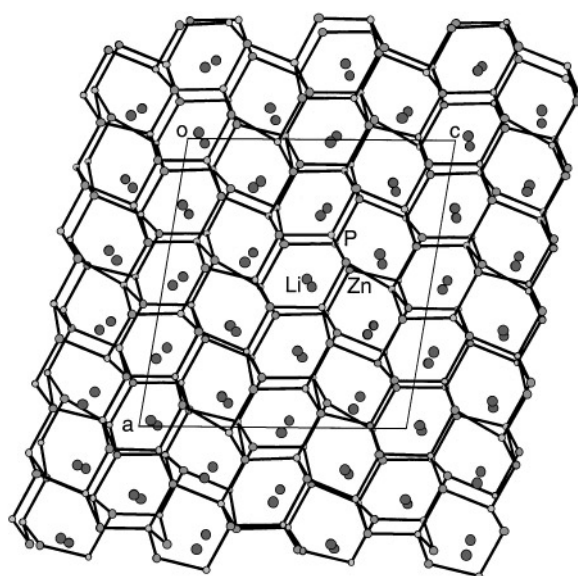


FIG. 3. The tetrahedral atom connectivity diagram showing the six-ring channels projected down the crystallographic b -axis.

sheets. In $\text{LiZnPO}_4\text{-CR1}$, the most prominent stacking direction is along the monoclinic c -axis. The interlayer distance along this direction is about 4.0 \AA .

For each tetrahedral atom in the layer, one bond serves to join two adjacent layers through the T–O–T linkage (T refers to tetrahedral atoms). For six T-atoms in each hexagonal ring, the interlayer bond is directed up and down alternatively (UDUDUD) in the cristobalite framework. This is similar to that observed in the tridymite family of structures. A systematic classification of different hexagonal sheets has been presented before (8).

$\text{LiZnPO}_4\text{-CR1}$ has channels with a window opening consisting of six tetrahedral atoms (Fig. 3). The extra-framework lithium cations are located near the center of these channels. Unlike the tridymite, ABW, and some other families of framework structures also constructed from hexagonal layers, the directions of the six-ring channels in $\text{LiZnPO}_4\text{-CR1}$ are significantly offset from the layer stacking directions because layers are staggered in projection (8). In $\text{LiZnPO}_4\text{-CR1}$, unique six-ring channels are found along the crystallographic $[010]$ and $[110]$ directions, respectively.

Six-membered rings are commonly found in zeolite-type structures. However, a framework structure with only 6-rings is always significantly more dense than zeolite-type structures. A possible reason is that without the help of 5-rings and 4-rings, 6-rings alone are unlikely to form closed cages similar to those cages observed in zeolites, such as α -cage, β -cage, γ -cage, and ε -cage (13). The lack of large voids enclosed in these types of cages contributes to the high framework density in structures with only 6-rings.

Comparison with Other Lithium Zinc Phosphates

Three other different polymorphs of LiZnPO_4 have been reported. The phenakite form has a completely different framework topology from $\text{LiZnPO}_4\text{-CR1}$ reported here (17). An orthorhombic form ($\delta_1\text{-LiZnPO}_4$) was also described as having the cristobalite topology (18,19). The $\alpha\text{-LiZnPO}_4$ has the same space group and similar cell parameters to the title compound and was classified as belonging to “tetrahedral structures” in the original report (20). Our study indicates that it also has the cristobalite-type topology. For convenience in comparison, the unit cell parameters of all four polymorphs are summarized in Table 4. Note that all four polymorphs are noncentrosymmetric, in support of research efforts in exploring these systems in search of useful physical properties such as SHG.

The differences between the three cristobalite polymorphs discovered so far include the differing extent of distortions from the ideal cubic symmetry. These distortions may be

TABLE 4
A Summary of Structural Parameters for Four Polymorphic Lithium Zinc Phosphates

Formula	Space group	a (\AA)	b (\AA)	c (\AA)	β ($^\circ$)
LiZnPO_4	$R3$	13.628	13.628	9.096	90
$\text{LiZnPO}_4\text{-CR1}$	Cc	17.296	9.775	16.199	98.95
$\alpha\text{-LiZnPO}_4$	Cc	17.250	9.767	17.106	110.9
$\delta_1\text{-LiZnPO}_4$	$Pna2_1$	10.019	4.966	6.675	90

reflected in differences in geometrical parameters such as T–O–T angles, which are known to be rather flexible in tetrahedral framework structures (8). Structures with the same framework topology but different crystal structures are very common in both dense- and open-framework structures. For example, all three common polymorphs of silica have α - and β -forms, such as α -quartz and β -quartz. The zeolite gismondine topology has been found to exist in more than 10 different space group symmetries (21, 6).

The fact that all four polymorphs of LiZnPO_4 consist of tetrahedral zinc indicates that Zn^{2+} has a strong preference for tetrahedral coordinations. The divalent metals in other ABCX_4 structures such as LiBPO_4 ($B = \text{Mg}^{2+}, \text{Co}^{2+}, \text{Fe}^{2+}, \text{Mn}^{2+}, \text{Ni}^{2+}$) all have octahedral coordinations. Most of these structures belong to the olivine-type family (2). The strong preference for tetrahedral coordination of Zn^{2+} compared to other divalent metals (except Be^{2+} , which is always tetrahedral) makes it an ideal choice in the designed synthesis of zeolite analog structures. So far, zeolite analog structures in the pure divalent metal phosphate system are only known to exist in the zinc and beryllium phosphate systems (22). By incorporating trivalent metals into cobalt, manganese, and magnesium phosphate systems, we have made numerous zeolite-type structures, some of which may have potential applications as molecular sieves (6,7). Based on the structural chemistry of Zn^{2+} that we have learned so far, it can be predicted that nearly all of those zeolite-type structures made in Mg^{2+} and Co^{2+} systems can probably be made with Zn^{2+} .

ACKNOWLEDGMENT

The authors would like to acknowledge the support of the National Science Foundation (DMR-9520971).

REFERENCES

1. F. Liebau, "Structural Chemistry of Silicates." Springer-Verlag, New York, 1985.
2. O. Muller and R. Roy, "The Major Ternary Structural Families." Springer-Verlag, New York, 1994.
3. A. F. Wells, "Structural Inorganic Chemistry." Oxford University Press, New York, 1986.
4. X. Bu, P. Feng, T. E. Gier, and G. D. Stucky, *Zeolites* **19**, 200 (1997).
5. P. Feng, X. Bu, and G. D. Stucky, *Angew. Chem., Int. Ed. Engl.* **34**, 1745–1747 (1995).
6. P. Feng, X. Bu, and G. D. Stucky, *Nature* **388**, 735–741 (1997).
7. X. Bu, P. Feng, and G. D. Stucky, *Science* **278**, 2080 (1997).
8. P. Feng, X. Bu, S. H. Tolbert, and G. D. Stucky, *J. Am. Chem. Soc.* **119**, 2497–2504 (1997).
9. P. Feng, X. Bu, and G. D. Stucky, *J. Solid State Chem.* **131**, 160–166 (1997).
10. P. Feng, X. Bu, and G. D. Stucky, *J. Solid State Chem.* **129**, 328–333 (1997).
11. X. Bu, P. Feng, and G. D. Stucky, *J. Solid State Chem.* **131**, 387 (1997).
12. J. P. Dougherty and S. K. Kurtz, *J. Appl. Crystallogr.* **9**, 145 (1976).
13. D. W. Breck, "Zeolite Molecular Sieves." John Wiley & Sons, New York, 1974.
14. T. E. Gier, X. Bu, Wang, S.-L., and G. D. Stucky, *J. Am. Chem. Soc.* **118**, 3039–3040 (1996).
15. M. I. Khan, L. M. Meyer, R. C. Haushalter, A. L. Schweitzer, J. Zubieta, and J. L. Dye, *Chem Mater.* **8**, 43–53, (1996).
16. X. Bu, T. E. Gier, and G. D. Stucky, *Acta Crystallogr. Sect. C* **52**, 14–16 (1996).
17. X. Bu, T. E. Gier, and G. D. Stucky, *Acta Crystallogr. Sect. C* **52**, 1601–1603 (1996).
18. T. R. Jensen, P. Norby, and P. C. Stein, *J. Solid State Chem.* **117**, 39–47 (1995).
19. W. T. A. Harrison, T. E. Gier, J. M. Nicol, and G. D. Stucky, *J. Solid State Chem.* **114**, 249–257 (1995).
20. L. Elammari and B. Elouadi, *Acta Crystallogr. Sect. C* **45**, 1864–1867 (1989).
21. W. M. Meier, D. H. Olson, and Ch. Baerlocher, "Atlas of Zeolite Structure Types." Elsevier, New York (1996).
22. T. E. Gier and G. D. Stucky, *Nature* **349**, 508–510 (1991).